

SPONTANEOUS EMISSION OF GRAVITY WAVES BY INTERACTING VORTEX DIPOLES IN A STRATIFIED FLUID: LABORATORY EXPERIMENTS

YAKOV AFANASYEV*

*Department of Physics and Physical Oceanography,
Memorial University of Newfoundland, St. John's, NF, Canada*

(Received 27 February 2003)

Results from a new series of experiments on the geophysically important issue of spontaneous emission of internal gravity waves during unsteady interactions of vortical structures are presented. Vortex dipoles are a common element of a quasi-two-dimensional turbulent flow. Vortex dipoles perform translational motion and can collide with other vortices. During collision events the flow is unsteady and unbalanced and a further adjustment process associated with these events can therefore result in the spontaneous emission of gravity waves. Our laboratory experiments demonstrate that gravity waves are emitted when two translating vortex dipoles interact (collide) in a layered fluid, in accord with the current theoretical results. The emission was evident both in a two-layer system and in a fluid with a linear distribution of density with depth. The waves were generated during the period of deceleration of the secondary dipoles which constitute a vortex quadrupole emerging immediately after the collision of the primary dipoles.

Keywords: Vortex dipoles; Internal waves; Geophysical turbulence

1. INTRODUCTION

Recent theoretical studies (Ford *et al.*, 2000; McIntyre and Norton, 2000) demonstrate that the ultimate limitations of such concepts in atmospheric and oceanic fluid dynamics as balance, slow-manifold, and potential vorticity inversion, are due to the weak emission of inertia-gravity waves by unsteady, vortical flows that are otherwise close to being in (quasi/semi) geostrophic balance. These concepts provide a theoretical basis for the separation of the flows into (balanced) vortical and wave components. The dynamics of the fluid system can therefore be essentially reduced to reconstruction of the vortical component only while the waves are neglected. The possibility of filtering out waves is of special importance in numerical models of the circulation of the ocean and atmosphere where wave activity is often considered only for parameterization of subgrid processes. It is therefore important to establish the exact circumstances through

*Tel.: (709) 737 2500. Fax: (709) 737 8739. E-mail: yakov@physics.mun.ca

which the wave emission takes place and to measure quantitatively the amount of energy radiated in these events.

Fundamental elements of geophysical turbulence are quasi-two-dimensional vortices such as monopoles, dipoles, and quadrupoles (Voropayev and Afanasyev, 1994). A vortex dipole in particular can be considered as the simplest vortex structure that performs self-induced translational motion and is therefore characterized by a net linear momentum. It is clear that for a volume of fluid to acquire momentum, a force must be applied to it. Thus, dipoles can be easily generated in a layered fluid when some localized forcing is applied. Dipoles can be generated in a stratified/rotating fluid either by external forcing or by internal processes such as, for example, baroclinic instability or breaking of Rossby waves. A remarkable property of vortex dipoles is their self-similarity which implies in particular that once the dipole is formed it does not have memory of peculiarities of initial conditions. The only control parameter is the integral amount of momentum transferred to a fluid by the source. The nature of forcing is therefore not important and we can disregard the details of the particular mechanism of generation and concentrate on the dynamics of the dipoles after they are formed. A simple laboratory experiment with a layered system, similar to the upper ocean where a thin layer of fluid lies on top of a thick heavier layer, demonstrates multiple dipoles (Fig. 1) when wind jets are blown over the surface of water. A dipole, once formed from the jet-like flow, then moves with almost constant speed, decelerating slowly due to viscous drag as well as entrainment of ambient quiescent fluid. The latter process increases the mass of the dipole decreasing its velocity due to the conservation of momentum. The empirical asymptotic model (Voropayev *et al.*, 1991) based on the conservation of mass and momentum can be used to describe the dipole in such a regime. If the Reynolds number of the flow is moderately high ($\sim 100\text{--}300$) the viscous boundary layer associated with the moving dipolar vortex (and the jet-like flow) is thin and the entrainment is negligible. An asymptotic steady solution known as the

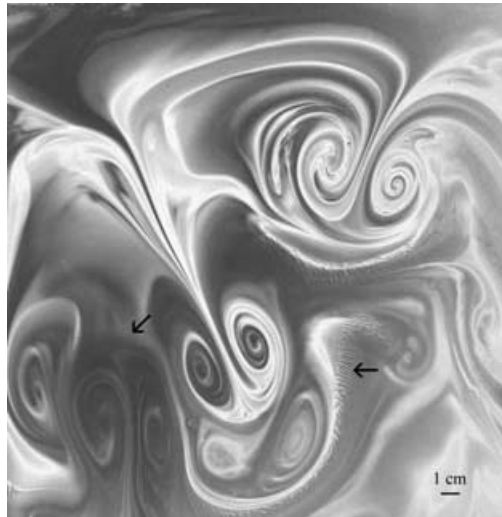


FIGURE 1 Photograph of the flow induced by chaotic forcing of a thin layer of fluid lying on top of the heavier layer. The flow consists of interacting vortex dipoles. The flow is visualized by pH-indicator in acid-base water solution. Arrows indicate the interactions of vortex dipoles.

Chaplygin–Lamb dipole (e.g. Meleshko and van Heijst, 1994) can be used to describe a dipole moving with constant speed in a nonviscous fluid. For even higher values of Re the flow becomes turbulent and the question arises as to whether the laboratory results can be applied to oceanic–atmospheric dipoles. The common argument in this context is that there is a gap in the energy spectrum between large-scale motion and small-scale turbulence. The idea of separation of length scales appears to be very fruitful providing the basis for the existence of coherent motions, i.e. large-scale ordered motions in the field of small-scale background turbulence. The coefficient of horizontal exchange of momentum due to the small scale eddies is very large and the effective Reynolds numbers for large-scale vortices are therefore moderate and are comparable to those in the laboratory.

The dipoles interact with each other as well as with solid boundaries (Afanasyev *et al.* 1988; Voropayev and Afanasyev, 1992). In Fig. 1, a few events of interactions between dipoles can be observed. During these elementary events of collisions/scattering or merging interactions the fluid parcels undergo accelerations and decelerations which are appreciable when compared to the slow decelerations of freely moving dipoles due to viscous friction and entrainment. Nonstationarity associated with the accelerations during interactions can provide appropriate conditions for spontaneous-adjustment emission. The term spontaneous is used here to distinguish this adjustment from the adjustment which occurs due to initial conditions, namely Rossby adjustment (Ford *et al.*, 2000; McIntyre and Norton, 2000). The initial conditions in our problem are created by some physical mechanism (forcing) which generates the vortex dipoles. Once the forcing is stopped and the dipoles are evolving freely, we consider the emission of gravity waves during this period as spontaneous. We report laboratory observations illustrating the mechanism of the spontaneous emission. For simplicity we herein concentrate on the flows in a stratified fluid without background rotation.

Rotation and stratification can both act to provide balanced vortical flows and to sustain waves. However, these effects are not required to act together and can be considered separately. Strongly stratified flows in particular can be separated in the leading order in Froude number into (quasi-) noninteracting vortical and wave components (Riley and Lelong, 2000). The vortices in a strongly stratified fluid (at a vanishing Froude number) often take form of lens-shaped “pancakes” in which the motion is predominantly horizontal. Theoretical considerations by Plougonven and Zeitlin (2002) demonstrate that the balanced but nonstationary pancake vortex permanently radiates internal gravity waves. Rotation can be involved when the particular mechanisms of generation of vortices are considered. In the laboratory experiments of Lovegrove *et al.* (2000) the baroclinically unstable flow in a two-layer rotating annulus was found to emit inertia-gravity waves. Rotation can be an important factor in determining the stability characteristics of vortices (e.g. Afanasyev, 2002) and can also affect the intensity of emission. According to Ford *et al.* (2000) “Coriolis effects can be expected to weaken the emission” but would “not... make it exactly zero, even for arbitrary small Rossby number.”

In a new series of experiments reported herein we chose to consider a flow different from those considered in previous theoretical and laboratory studies. In particular, we provide an external mechanism for the controlled generation of vortices rather than relying on the instability of the basic flow to create an unsteady vortical flow. Since in a context of geophysical turbulence it is of interest to experimentally examine the emission of waves by strongly interacting vortices (dipoles) rather than that by a

slowly evolving noninteracting vortex, we will consider the emission that occurs during the collision of two dipoles.

2. LABORATORY APPARATUS AND TECHNIQUE

Our experiments were carried out in a rectangular glass tank of horizontal dimensions 30×40 cm and of height 10 cm. The tank itself was filled with a linearly stratified or two-layer fluid. The two bucket technique was used to create a linearly stratified fluid with a buoyancy period $T=3-6$ s. In the case of a two-layer fluid the lower layer was of thickness 1 cm and the upper layer of thickness 2 cm. The difference in the concentration of salt between the layers was 5 g/L. The lower layer was filled carefully from a nozzle at the bottom of the tank to avoid mixing between the two layers although some mixing was unavoidably introduced during the experiments. The thickness of the mixed interface between the layers however was within the range of 1–3 mm. The horizontal velocity field in the flow was measured using a Particle Image Velocimetry (PIV) technique. A description of the method and general technique is given by Fincham and Spedding (1997) and Pawlak and Armi (1998). We used a 1 W Argon laser to illuminate a horizontal plane in the flow. The seeding particles were polyamid spheres of mean diameter $50 \mu\text{m}$. To measure the variation of thickness of the layers in some experiments, dye was introduced at the interface between the layers. The dyed interfacial layer was then illuminated by the laser at an oblique angle. The interface was visible due to the scattering of light by the dye. Images from a video recording of the flow were then processed digitally by subtracting the consecutive images of the flow from each other with 1 s interval to eliminate the background and to show only the regions of the flow where the unsteady motion takes place. This procedure is in fact equivalent to differentiation with respect to time.

The dipoles in the experiments with linearly stratified fluid were generated by an impulsive injection of fluid at its equilibrium density level at approximately the mid-depth of the layer. A jet injected for a short period of time $\Delta t=2-5$ s transports a horizontal momentum $\rho J=4\rho q^2 \Delta t/\pi d^2$ into the fluid. Here ρq is the mean mass flux at the nozzle exit, whose diameter is $d=0.2$ cm. The quantity J is the main governing parameter which characterizes the source and the dipole generated by the source (e.g. Voropayev and Afanasyev, 1994). A typical value of this parameter in our experiments is $J=10^2 \text{ cm}^4 \text{ s}^{-1}$.

An electromagnetic method was used in the experiments with two-layer fluid to reduce the initial perturbations. Two permanent magnets of 1.8 cm in diameter and 0.5 cm in height were placed at the bottom of the tank so that their magnetization axes were oriented vertically (Fig. 2). Each magnet produces a magnetic field with a vertical component of approximately 0.09 T. An electric current of magnitude 3 A was then maintained in the horizontal plane between two electrodes placed at the sides of the tank. The interaction of the magnetic field with the electric current results in a horizontal ampere force exerted locally on the fluid in the direction perpendicular to the electric current. The localized force generates a vortex dipole (Voropayev and Afanasyev, 1994). Thus, the two magnets generate vortex dipoles directed toward one another. A similar electromagnetic technique has been used extensively in experiments on two-dimensional turbulence in thin layers of electrolytic fluid (e.g. Hansen *et al.*, 1998; Danilov *et al.*, 2002).

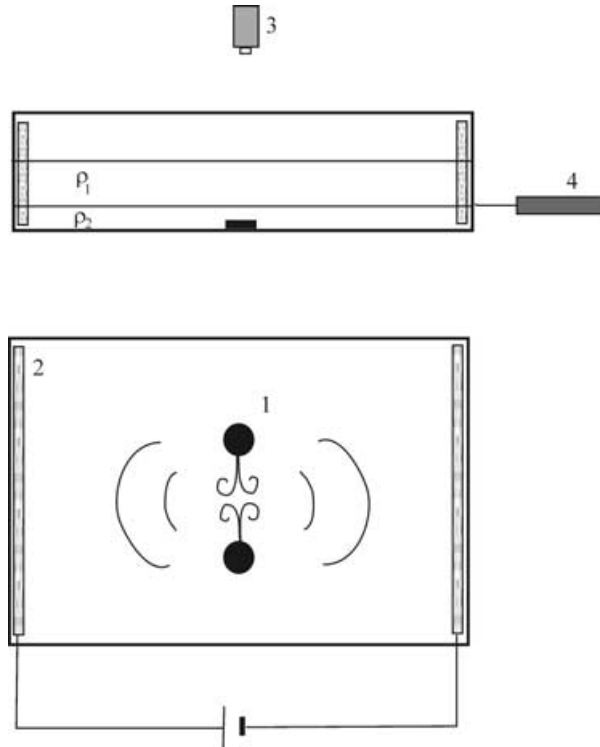


FIGURE 2 Sketch of the experimental setup. Two permanent magnets (1) are placed at the bottom of the tank between the electrodes (2). The fluid consists of two layers of salt water of density ρ_1 and ρ_2 . The top view of the flow is recorded by the video camera (3). The interface containing dye or seeding particles is illuminated by the laser (4).

A typical value of the momentum flux delivered by each magnet to the fluid was $I = 0.15 \text{ cm}^4 \text{ s}^{-2}$. This value cannot be obtained directly from the velocity field measured by PIV method because the exact vertical distribution of horizontal velocity is not known so it is not possible to perform integration over the entire volume of fluid. The value of I , however, can be obtained indirectly with reasonable accuracy using the results of the previous extensive studies on the dynamics of the vortex dipoles (Afanasyev *et al.*, 1989; Voropayev *et al.*, 1991; Voropayev and Afanasyev, 1994). Here we use the property of self-similarity of these flows. In particular the width D of the dipole is proportional to its length L , $D = \alpha L$ at any time during the growth of the dipole and neither of the dimensions of the dipole are sensitive to initial conditions. In particular, this means that the size of the dipole does not depend on the diameter of the magnet once the dipole is formed. The coefficient of proportionality α is a function of a single control parameter, namely the nondimensional intensity of the source I/ν^2 , where ν is the kinematic viscosity of the fluid. This function is well documented for a wide range of the variation of its argument. Simple measurements of the dimensions of the dipole during the action of the source allows us to obtain the value of α and therefore to find the value of I/ν^2 using the plot $\alpha(I/\nu^2)$ in Fig. 5.6 in Voropayev *et al.* (1991). It can be also shown that the Reynolds number of the flow can be defined as $\text{Re} = (I/\nu^2)^{1/2}$. A typical value of I/ν^2 in our experiments was $I/\nu^2 = 1500$ which gives $\text{Re} = 40$.

The current used for the generation of dipoles in our experiments was maintained for a short period of time ($\Delta t = 3\text{--}5\text{ s}$). The total momentum delivered by the source to the fluid is therefore $J = I\Delta t = 0.45\text{--}0.74\text{ cm}^4\text{ s}^{-1}$. These values are much less than the values of the total momentum delivered by the source when the injection of fluid was used to generate dipoles. Since the magnetic field of the magnet decays rapidly with distance from the magnet, the flow was effectively induced only within approximately 1 cm above the magnet. The flow was therefore concentrated approximately at the interface between two layers of different density. The dipole is essentially a lens-shaped flow (“pancake”). The vertical size of the dipole increases during the action of the source and remains approximately constant after the source stops (Afanasyev and Voropayev, 1989). Measurements of the vertical size H_{flow} of the dipoles using dye streaks give $H_{\text{flow}} = 1.5\text{--}2\text{ cm}$ with approximately parabolic distribution of horizontal velocity within the lens.

3. RESULTS AND INTERPRETATION OF THE EXPERIMENTS

The first series of experiments was conducted in a fluid with linear distribution of density in the vertical direction. Dipoles were generated by the impulsive horizontal injection of a small volume of fluid at its equilibrium density. The injection produces an initially turbulent jet-like flow which rapidly adjusts to horizontal motion due to the buoyancy force and forms a propagating vortex dipole. The experiments demonstrate that a strong initial injection generates an internal wave of significant amplitude (Fig. 3A). To measure the phase speed and the wavelength of the wave, it is convenient to use the Hovmoller diagram of the flow (Fig. 4). This diagram represents

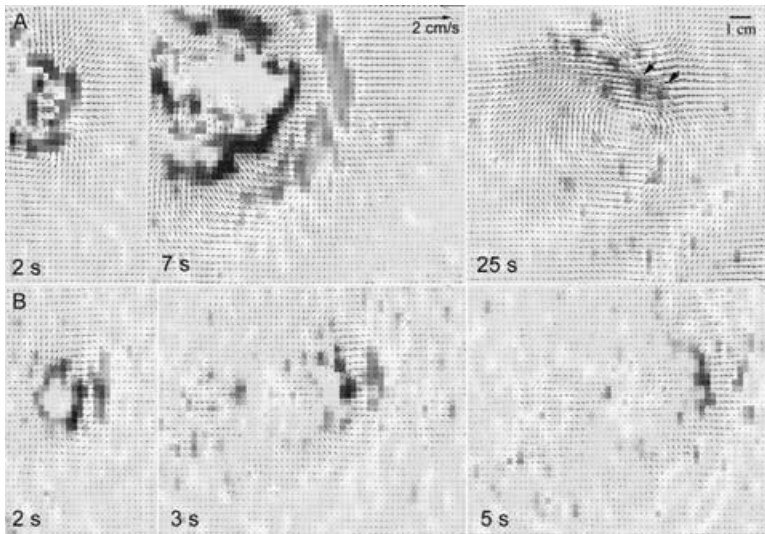


FIGURE 3 Flow maps showing the divergence of the horizontal velocity field where the divergence or convergence of velocity indicate a crest or a trough of the wave respectively. (A) Strong initial injection in a linearly stratified fluid. The velocity field is measured on a plane that is 0.5 cm above the central plane of the flow. The two arrows in the last panel indicate the regions of low and high pressure in the dipole. (B) Weak injection, the plane is 2.2 cm above the central plane of the flow.

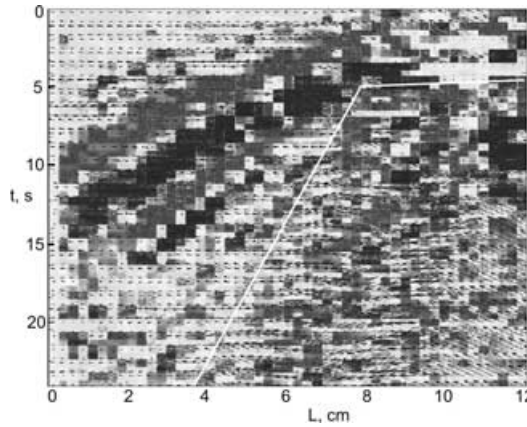


FIGURE 4 Hovmoller diagram of divergence of horizontal velocity along the axis of the dipole for the experiment shown in Fig. 3(A). The solid line shows the propagation of the front of the vortex dipole formed after the initial collapse.

the temporal variation of the flow along the axis of propagation of the dipole for the experiment shown in Fig. 3(A). The narrow regions of the images along the axis were cropped and then combined in a vertical stack to form the Hovmoller diagram. Distinct crests and troughs of the wave can be clearly observed as a succession of red and blue lines. The speed of propagation of constant phase, c , can be easily measured as the slope of the lines which gives the value of $c = 0.6 \pm 0.03$ cm/s. The half-wavelength can be measured as the distance between the red and blue lines in the horizontal direction. The values of the horizontal wavelength obtained for the most distinct lines are $\lambda = 4.0 \pm 0.4, 3.2 \pm 0.3, 2.2 \pm 0.2$ cm. The period of the wave, $T = \lambda/c$, can then be estimated to be 6.7, 5.3, 3.7 s. It is interesting to note that the period of the waves in the tail of the wave envelope is within experimental accuracy equal to the buoyancy period, $T_b = 3.8$ s for this particular experiment. The waves in the tail are therefore almost vertical oscillations at the buoyancy frequency.

A localized injection is equivalent to the action of a force concentrated in a small volume of fluid. If one considers (e.g. Voropayev and Afanasyev, 1994) a planar flow induced by a force $\rho \mathbf{f}(\mathbf{x}, t)$ (force per unit area of unit thickness) that acts on the fluid inside a small area $S(\mathbf{x})$, the far-field of pressure is given by

$$\frac{p}{\rho} = \frac{1}{2\pi} \frac{d\mathbf{J}}{dt} \cdot \frac{\mathbf{x}}{|\mathbf{x}|^2},$$

where \mathbf{J} is the total impulse applied by the force distribution since the onset of the motion

$$\mathbf{J} = \int_0^t dt \int_S \mathbf{f}(\mathbf{x}, t) dS.$$

One can also show (e.g. Saffman, 1992; Voropayev and Afanasyev, 1994) that half of the applied impulse ends up in the momentum of the fluid while the remaining half goes to building the appropriate pressure field. The distribution of pressure is of a dipolar type, $p \propto \cos \theta$, where θ is the polar angle measured from the direction of the vector \mathbf{J} .

The initial flow, consisting of the jet injected from the nozzle and the entrained fluid, is turbulent. The distribution of density in the vertical direction is also perturbed because of the buildup of high pressure associated with the rapid deceleration of fluid after the injection. The three-dimensional perturbations are then effectively suppressed by buoyancy and the vertical collapse of the flow can be characterized as the initial adjustment of the flow. Intense emission of the gravity waves is associated with this adjustment. Strictly speaking this emission cannot be considered as a spontaneous emission since it occurs due to the initial adjustment. The wave generated during the initial adjustment eventually propagates ahead of the dipole which is formed as a result of the adjustment. The region occupied by the dipole is marked by a solid line in Fig. 4. The dipole is formed after the initial collapse and is distinguished by the large velocity arrows in the diagram. It is clear from Fig. 4 that it is the initial adjustment (collapse) that generates the most intense wave. The dipole then performs translational motion with almost constant speed, decelerating slowly due to viscous drag as well as entrainment of the ambient quiescent fluid. An almost steadily propagating dipole can be associated with the region of low pressure in its center and the region of high pressure at the front (the last panel of Fig. 3A). The dipole therefore generates an internal wave which is steady in the frame of the moving dipole (Fig. 3B). The half-length of the wave in the horizontal plane corresponds to the distance between the high and low pressure regions in the dipole (approximately half of the longitudinal extent of the dipole). Due to deceleration the dipole emits internal waves which propagate upstream. These waves, however, are much weaker than the initial wave. Further experiments in which the head-on collisions of two dipoles were reproduced, demonstrated the emission of internal waves after the collision for different values of intensity of the sources. However, since the flow was initially turbulent, these collisions were not reproduced with confidence, and the quantitative data on temporal and spatial characteristics of the waves and the flow contain significant scatter. Another disadvantage of the experiments with turbulent injection is that the most significant emission of waves occurs due to the initial adjustment. Although these experiments do demonstrate qualitatively the emission of waves by a decelerating dipole, a different experimental technique was adopted in order to more clearly demonstrate the emission during the spontaneous adjustment event, namely the interaction of dipoles.

To achieve a laminar regime of the flow from the very start the electromagnetic method was used for the second series of experiments. In these experiments the dipoles were generated using permanent magnets. The thickness of the layer occupied by the flow was limited due to the limited vertical extent of the magnetic field. This allowed us to use a more shallow layer of fluid. A two-layer stratification was used in these experiments instead of a linear stratification. Figure 5 shows a typical development of the flow visualized by dye. When two primary dipoles collide they form two secondary dipoles in the perpendicular direction. This process can be characterized as the formation of a vortex quadrupole (Voropayev and Afanasyev, 1994). In its archetypal form, a quadrupole is formed under the action of two equal forces of opposite directions located close to each other (force dipole). The intensity of the source is characterized by the quantity $Q = \varepsilon J$, where ε is the distance between the two forces of magnitude ρJ . The spatial distribution of pressure (and vorticity) in the quadrupolar flow is proportional to $\cos 2\theta$.

The emergence of the secondary dipoles cause a significant emission of waves. These waves are evident in Fig. 6 as a succession of light and dark areas at the front of the

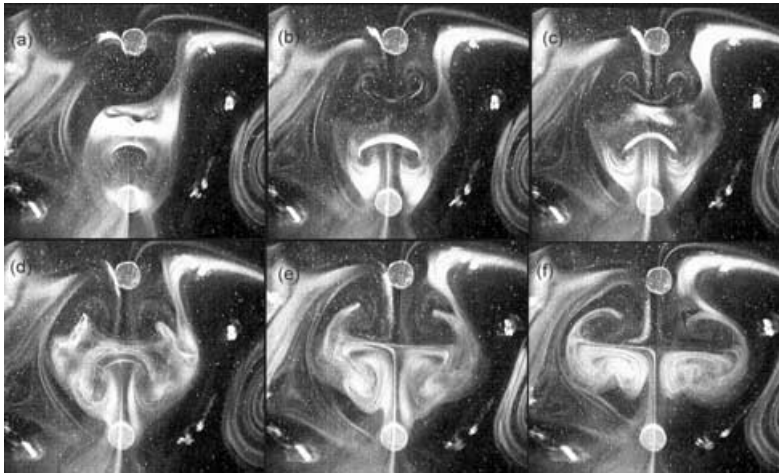


FIGURE 5 Succession of images showing the formation of the vortex quadrupole as a result of the collision of two dipoles, $t = 6$ (a), 9.2 (b), 10.8 (c), 13.6 (d), 18.8 (e), 26.6 s (f). The dipoles are induced by the electromagnetic method near the interface between two layers of different density. Patches of dye were introduced at the interface to visualize the flow. The spatial scale of the images is represented by the size of the magnets (diameter 1.8 cm).

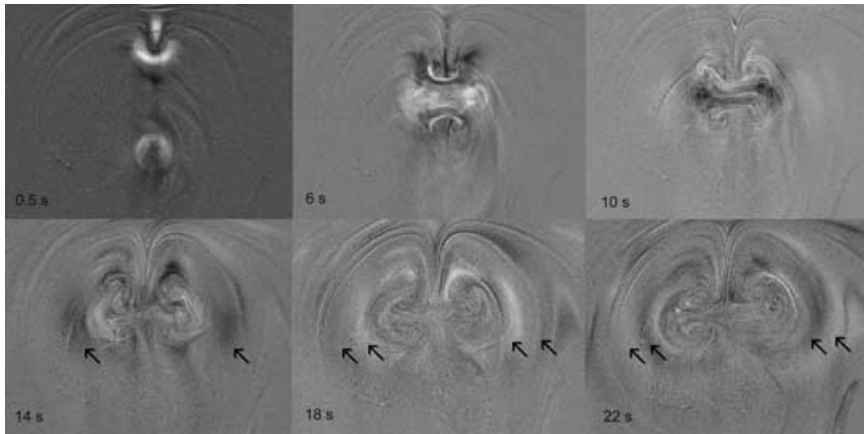


FIGURE 6 A succession of images showing the modulation of the thickness of the dyed layer of fluid. The images were obtained by subtraction of successive video frames similar to those shown in Fig. 5 with 1 s interval. Arrows show the propagation of peaks and troughs of the wave.

developing secondary dipoles. The images in Fig. 6 were obtained by subtracting from each image of the flow the previous image in 1 s intervals. Images similar to those shown in Fig. 5 but with more uniform initial distribution of dye were used for subtraction. Since waves modulate the thickness of the dyed layer, the subtraction allows us to see where the thickness changes with time with respect to its background level. The maximal amplitude of the waves is in the direction of the translation of the secondary dipoles. Note, that the flow itself is unsteady and creates density perturbations which modulate the thickness of the dyed layer. In Fig. 6 these perturbations typically look like fine-scale features which are mostly located in the regions of the jets and at the front of dipoles.

To obtain a more complete picture of the angular and radial distribution of the wave, subtracted images similar to those shown in Fig. 6 were transformed such that the horizontal axis represents polar angle θ while the vertical axis represents radial distance r from the center (symmetry point for the colliding dipoles). The result of this transformation is demonstrated in Fig. 7(b). Pixel intensity of the image as a function of polar angle θ for any particular radius r can then be easily plotted. An example is given in Fig. 8 for the radial distance $r=185$ pixels (line in Fig. 7b) and compared with the function $A\cos[2(\theta+\theta_o)]$, where $\theta_o=15^\circ$ and the amplitude A is arbitrary. A small angular shift θ_o is introduced here to account for the slight asymmetry of the collision of the dipoles. As a result of this asymmetry the secondary dipoles move along a line which is not exactly perpendicular to the line of motion of primary dipoles. The line $r=185$ pixels in Fig. 7(b) intersects the regions where the wave is more pronounced (at approximately 180 and 360°) as well as the regions of the jets in the perpendicular direction. The jets contain perturbations of intensity due to the relatively strong unsteady flow in these regions. These perturbations are not due to the wave and they contaminate the data giving nonzero intensity in between the maxima in the plot in Fig. 8. Although the scatter is significant, Fig. 8 demonstrates that the distribution

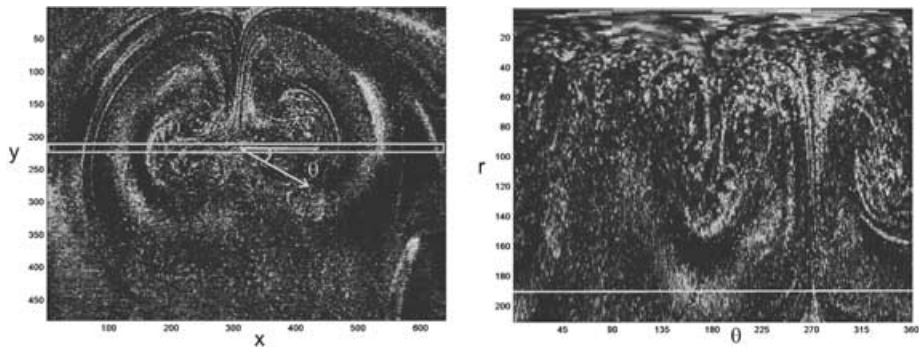


FIGURE 7 A subtracted image of the flow in Cartesian coordinates and the same image transformed into polar coordinates. (a) The rectangular region of the flow corresponds to the area cropped to generate the Hovmöller diagram of the flow (Fig. 9). (b) The horizontal line indicates the particular radius for which the variation of the pixel intensity with polar angle was plotted (see Fig. 8).

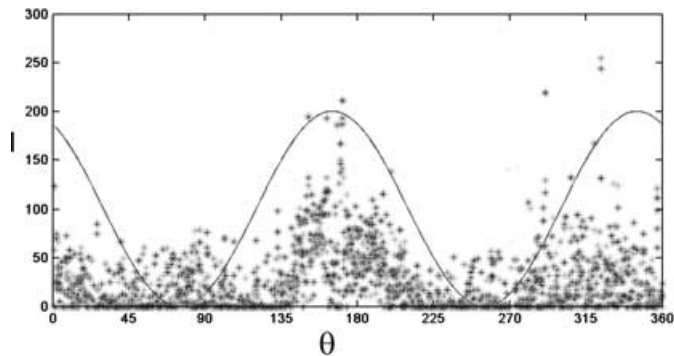


FIGURE 8 Variation of pixel intensity with polar angle averaged for the distances between 188 and 191 pixel from the center of the collision of dipoles. Intensity is represented by the values between 0 and 255. The solid line represents the function $A\cos[2(\theta+\theta_o)]$ where $\theta_o=15^\circ$ and the amplitude A is arbitrary.

of the amplitude of the wave with θ has two distinct maxima. The distribution of the amplitude of the wave is therefore of approximately quadrupolar character similar to the distribution of velocity and pressure in the vortical flow as one could expect.

The Hovmoller diagram of the flow (Fig. 9) represents the temporal variation of the flow along the axis of propagation of secondary dipoles. Similar to the diagram in Fig. 4 it is composed of narrow regions of the images which were cropped (cropped area is shown by a rectangle in Fig. 7a) and then combined in a vertical stack. The insert in Fig. 9 represents the same diagram where the essential features were enhanced for clearer illustration of the discussed features of the flow. The diagram in Fig. 9 demonstrates four distinct waves (labeled by Numbers 1–4) which can be clearly observed as the succession of light and dark lines. The speed of propagation of constant phase, c , is measured to be $c = 0.8, 0.6, 0.5$ cm/s for the waves 1–3 respectively. The distance between lines 1–4 changes with time which indicates that the wavelength of the waves can be measured only approximately. For the first wave, the mean wavelength was estimated to be approximately $\lambda = 4.5$ cm. The waves are emitted from the front (labeled by the number 5 in the diagram) of the propagating secondary dipoles which decelerate. Note that the velocity of dipoles, when the source (the forces) acts continuously, decays as $U \propto t^{-1/2}$, and, when the source acts impulsively for a short period of time and then stops, it decays as $U \propto t^{-2/3}$ (Voropayev and Afanasyev, 1994). This scaling is based on the integral models which take into account the balance of momentum and mass (including the mass entrained into the flow from the viscous boundary layer) for dipoles in a stratified fluid. The scaling is in a good agreement with experimental data. In both regimes, the dipoles decelerate. Line 5, which represents the front of the dipole, is therefore curved in contrast to the straight lines representing the waves propagating with constant speed. It is interesting to note that the straight lines are approximately tangent to Line 5. This indicates that the phase speed of the waves matches the current speed of the dipoles at the moment when each wave is generated. The emission of waves is most intense immediately

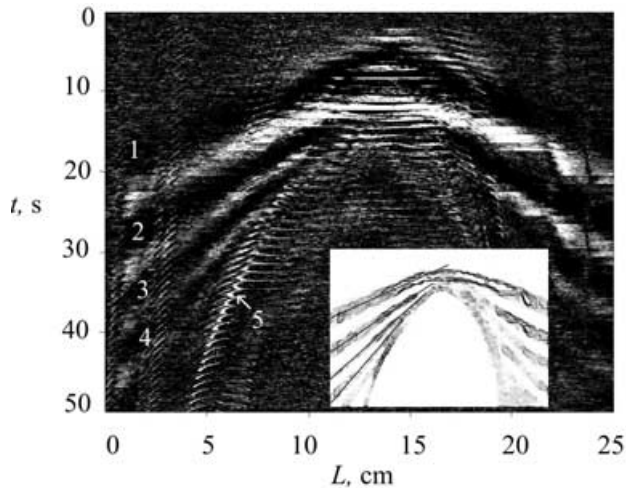


FIGURE 9 Hovmoller diagram composed of subtracted images of the flow along the axis of secondary dipoles for the experiment shown in Fig. 6. Numbers 1–4 indicate the lines of constant phase, while 5 shows the position of the front of the developing secondary dipoles. The insert shows the same diagram processed with contour enhancing software.

after the collision, during the time interval between 10 and 15 s. This interval corresponds to the process of formation of secondary dipoles which also includes the vertical collapse of the flow after the collision.

The phase speed and group speed of linear interfacial waves can be obtained from the relevant dispersion relationship

$$\omega^2(k) = \frac{\rho_2 g' k}{R_1 + R_2}, \quad (1)$$

where ω is the angular frequency, ρ_i is the density of the upper and lower layers (with $i=1$ and 2 , respectively), k is the wavenumber, $R_i = \rho_i \{\cotanh(kh_i)\}$, $g' = g(\rho_2 - \rho_1)/\rho_2$ is the reduced gravity, and g is the gravitational acceleration. The phase speed c_p and the group speed c_g calculated for the values of the parameters of this particular experiment are shown in Fig. 10 as functions of the wavelength $\lambda = 2\pi/k$. One can use the graph in Fig. 10 to check the consistency between the speed and the wavelength of the waves observed in the experiments. If one considers the succession of waves in Fig. 9 as a wave envelope the speed of the front of the envelope (given by the slope of the first line) can be associated with group velocity $c_g = 0.8 \pm 0.1$ cm/s. The theoretical value of the group velocity for $\lambda = 4.5$ cm is $c_g = 0.7$ cm/s which is consistent with the experimental value.

Measurements of the position of a point at the front of the developing secondary dipole (Fig. 11a) allow us to obtain the velocity of the dipole (Fig. 11b) for different periods of its evolution. Two distinct regimes of flow evolution are evident. A peak in the velocity distribution characterizes acceleration and deceleration during the event of collision while the almost constant velocity after the collision represent the slowly decelerating dipoles. A short period of collision is characterized by a high average velocity ~ 1 cm/s, while the subsequent long period is characterized by a low velocity ~ 0.15 cm/s. A rapid deceleration of the dipoles was observed during the period between approximately 10 and 15 s. It is during this period that the most intense emission of gravity waves takes place (see Fig. 9). During this short period the velocity of the dipole was such that it was close to the phase speed of a wave whose wavelength

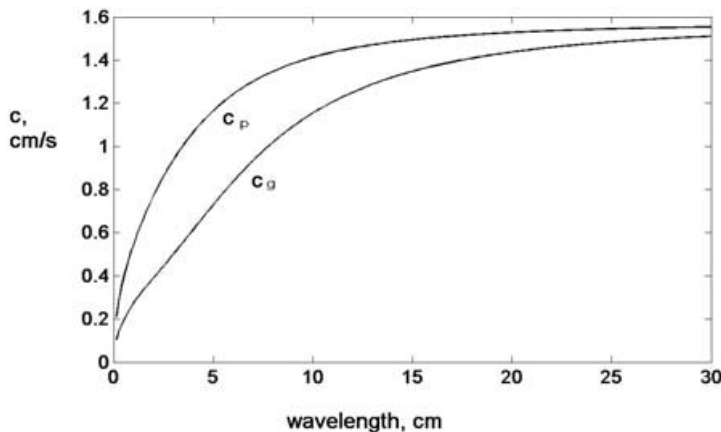


FIGURE 10 Phase speed and group speed of the interfacial wave for different values of the wavelength calculated from the dispersion relation (1).

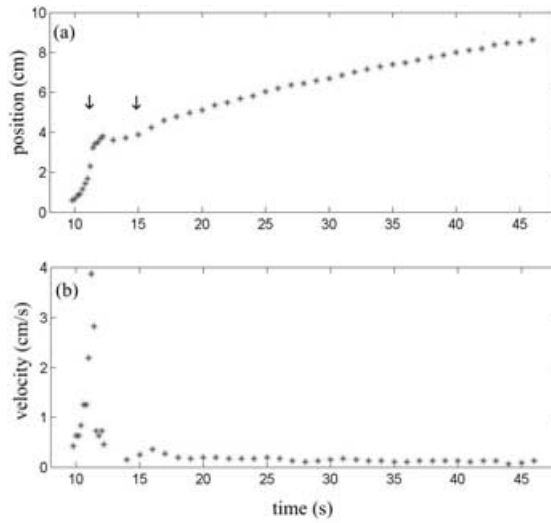


FIGURE 11 Position (a) and velocity (b) of a point at the front of one of the dipoles that emerge as a result of collision. The arrows indicate the period of rapid deceleration of the dipoles which is associated with the most intense emission of waves.

corresponds to the length of the dipole. Thus, both the velocity and the size of the dipole were optimal for the generation of the wave. After the transition to the second, slow-velocity regime, the wave moves ahead of the dipole.

For the purpose of comparison of the laboratory flow with atmospheric or oceanic flows it is useful to introduce Froude number $F = U/c$, where U is the speed of the dipole. The Froude number is of order unity immediately after the collision and then falls to a value of approximately 0.1–0.2.

An important question associated with the problem of wave emission by vortical flows is the determination of how much energy is emitted relative to the total energy of the flow. To estimate the energy of the wave, variations in the horizontal distance between two close points in the interface between the layers were measured. This distance changes periodically (Fig. 12) when the wave modulates the thickness of the layers, performing approximately three full oscillations of appreciable amplitude for the particular experiment in Fig. 12. The amplitude of the vertical displacement of the interface can then be easily estimated. The horizontal displacement of a particle at the interface for a progressive wave is given by the expression (e.g. Kochin *et al.*, 1948)

$$x = x_0 - A \frac{\cosh(kH)}{\sinh(kH)} \sin(kx_0 - \omega t),$$

where A is the amplitude of the vertical displacement of the interface and $H = 1$ cm is the thickness of the lower layer. For a distance l between two points at the interface one can obtain an approximate expression

$$\frac{l_{\max} - l_{\min}}{l} = 2Ak \frac{\cosh(kH)}{\sinh(kH)},$$

assuming that $kl \ll 1$.

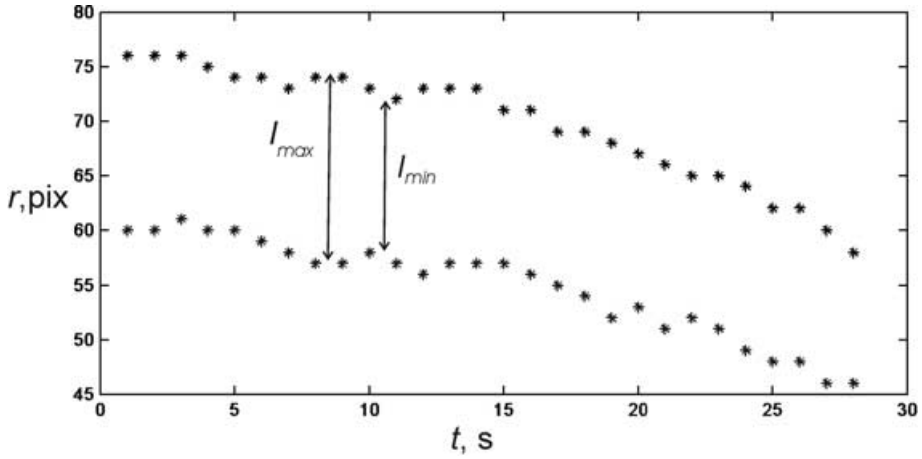


FIGURE 12 Variation of the positions of two points with time during the passage of the wave. The minimal and maximal distances between the points are indicated. The position is in pixels, 1 cm = 28 pixels.

For the experiment similar to that shown in Fig. 6, the relative length between two points located near the axis ($\theta = 180^\circ$) of the dipoles at a distance $r = 10.7$ cm from the collision center was measured to be $(l_{\max} - l_{\min})/l = 3/15$ (Fig. 12). This allows us to estimate the value of the amplitude of the wave to be approximately $A = 0.075$ cm. Implying that the wave amplitude varies in a quadrupolar manner ($\sim \cos 2\theta$) with azimuthal angle in the horizontal plane, the potential energy stored in the wave per wavelength can be estimated as following

$$P_w = \frac{1}{4} \pi r \lambda \rho_2 g' A^2 \quad (2)$$

which gives the value $P_w \sim 0.9 \text{ g cm}^2/\text{s}^2$. For the three full oscillations that were observed in the experiment we obtain the total potential energy of the wave field to be $1.8 \text{ g cm}^2/\text{s}^2$.

The total kinetic energy per unit depth of the flow can be obtained by direct integration over the entire area of the flow

$$E = \int \int \rho \frac{V^2}{2} dx dy$$

where ρ is the mean density and V is the velocity field at the interface. To measure the velocity field an experiment with seeding particles was performed. The parameters of the experiment were the same as in the experiments with the dyed flow. Assuming that velocity V varies parabolically with depth (similar to plane Poiseuille profile) and the value of velocity is maximal at the interface, we can obtain the total kinetic energy of the flow in the form

$$K = \frac{8}{15} E H_{\text{flow}},$$

where H_{flow} is the effective thickness of the flow. The assumption of the parabolic velocity profile was proven to work well even for more complex flows, namely quasi-two-dimensional turbulent flows, which consist of many interacting vortices and dipoles (e.g. Hansen *et al.*, 1998) and it is reasonable to use it for this simpler case. It was shown in the experiments with vortex dipoles generated by an impulsive action of the momentum source in both the linearly stratified fluid and the two-layer fluid that the typical vertical scale H_{flow} of the dipole remains constant after the dipole has been formed (Afanasyev and Voropayev, 1989). The appropriate dependence of H_{flow} on the main control parameters of the flow can be found on dimensional grounds as follows

$$H_{\text{flow}} = \gamma \left(\frac{J^2}{g'} \right)^{1/7}$$

This formula provides a good description of the experimental data if the value of the nondimensional coefficient is taken to be $\gamma = 1.2$. Taking the value of $J = 0.15 \text{ cm}^4 \text{ s}^{-1}$ we obtain $H_{\text{flow}} = 0.9 \text{ cm}$. This value however is lower than that obtained by direct measurements of H_{flow} using the dye streak method. This difference can be explained by the fact that the flow initially occupied a layer that had a height of approximately 1 cm above the magnets. Further entrainment of fluid contributed to the increase of the initial thickness. In this estimate we use instead the measured value of $H_{\text{flow}} = 2 \text{ cm}$. Using then the experimental value of $E = 60 \text{ g cm}^2/\text{s}^2$ we obtain an estimate for the kinetic energy of the dipole $K = 64 \text{ g cm}^2/\text{s}^2$. Assuming further that for both the wave and the dipoles their kinetic energy is equal to their potential energy, we obtain that approximately 4% of the total energy of the flow is radiated with the waves during the adjustment after the collision. Since the above estimate of the fraction of energy of the flow radiated is important, it is useful to perform an analysis of errors. The main experimental error, which comes from measurements of the variation of the distance between two points, is approximately 0.5 pixel. This results in a 20% error for the amplitude and a 40% error for the energy of the wave. The quantity E is measured with a 25% error and an additional error of 50% comes from the estimate for H_{flow} . Overall error for the fractional energy is therefore 70%.

4. DISCUSSION

The experiments reported in this article demonstrate the spontaneous emission of gravity waves during the collision of two vortex dipoles. The energy radiated away is a relatively small fraction of the total energy of the flow. Emission occurs when two secondary dipoles that appear as a result of the collision of two primary dipoles, rapidly decelerate (Fig. 11). The exact mechanism of emission is important especially in establishing the relevance of the results of these experiments to atmospheric flows. In this context it is necessary to clarify the role of viscosity in the dynamics of the flow. Molecular viscosity is one of the main control parameters of the flow in the laboratory. In particular, it defines the rate of entrainment of ambient fluid into the dipole and therefore controls the growth of its dimensions. The Reynolds number of the flow however is in the range $\text{Re} \sim 50\text{--}100$ and is much greater than unity. Thus, although

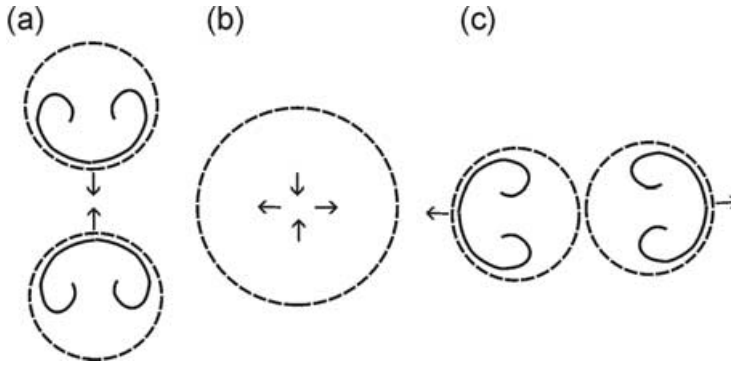


FIGURE 13 Sketch of the process of collision of two dipoles. Two primary dipoles moving head-on (a) collide forming a region of fluid with enhanced pressure in the center (b). The result of the collision is two secondary dipoles (c) moving away from the center in a direction perpendicular to that of the primary dipoles.

the influence of viscosity is important it is not dominant in the dynamics of the laboratory flows. Note, that similar mechanisms of entrainment controlled by turbulent or eddy viscosity rather than molecular viscosity work in atmospheric flows. During the collision viscous effects are even less important and can be disregarded since the event of collision is relatively short and there is no significant entrainment during this event. The collision of two dipoles is shown schematically in Fig. 13. The typical time of the collision event (intermediate stage in Fig. 13b) when the flow reorganizes and the secondary dipoles appear in the perpendicular direction is approximately 2–3 s for the laboratory flow (the width of the peak of velocity in Fig. 11b). The secondary dipoles acquire velocity U during the time interval Δt when the pressure force acts in the center of collision of the primary dipoles. If the primary dipoles move with velocity U just before the collision, the pressure can be estimated as $p = \rho U^2/2$. The process of collision is in fact equivalent to the action of a localized force in the center. The impulse of the pressure force changes the momenta of the secondary dipoles according to the relation $F_p \Delta t = mU$. The pressure force F_p is approximately equal to pLH where L and H are the horizontal and vertical scales of the dipoles. Taking the mass m of each dipole to be $m = \rho HL^2$ and disregarding the constant factors of order of unity, we get a simple estimate for the characteristic time of collision of the vortex dipoles in the form $\Delta t \approx L/U$. This estimate is independent of viscosity and can be applied both to the laboratory and geophysical flows. After the fast stage of the flow development, the regime changes such that the secondary dipoles move in opposite directions without significant interaction. They decelerate slowly due to viscous entrainment and friction.

Another factor is necessary for emission, namely that the parameters of the flow during rapid deceleration are such that the Froude number of the flow is $O(1)$. This factor, together with the rapid deceleration of dipoles provide a condition for the emission of gravity waves. A further required step in the analysis of the spontaneous emission of gravity waves clearly involves an investigation of the effects of rotation. Experiments with flows on a rotating platform are underway and will be reported elsewhere.

Acknowledgments

The author is indebted to Dr. M. I. McIntyre for suggesting the idea of the experiments reported in this article. This study has been supported by the Natural Sciences and

Engineering Research Council of Canada under grants 228941-2000 and 227192-2000, Canadian Foundation for Innovation and Canada/Newfoundland Comprehensive Economic Development Agreement.

References

- Afanasyev, Ya.D., "Experiments on instability of columnar vortex pairs in rotating fluid", *Geophys. Astrophys. Fluid Dynam.* **96**, 31 (2002).
- Afanasyev, Y.D. and Voropayev, S.I., "A model of the mushroom-like currents in a stratified fluid at the source of momentum acting impulsively", *Izvestiya Russ. Acad. Sci., Atmos. Ocean Phys.* **25**, 843 (1989).
- Afanasyev, Y.D., Voropayev, S.I. and Filippov, I.A., "Laboratory investigation of flat vortex structures in a stratified fluid", *Dokl. Akad. Nauk. SSSR* **300**, 704 (1988).
- Danilov, S., Dolzhanskii, F.V., Dovzhenko, V.A. and Krymov, V.A., "Experiments on free decay of quasi-two-dimensional turbulent flows", *Phys. Rev. E* **65**, 036316 (2002).
- Fincham, A. and Spedding, G., "Low cost, high resolution DPIV for measurement of turbulent fluid flow", *Exps. Fluids* **23**, 449 (1997).
- Ford, R., McIntyre M.E. and Norton, W.A., "Balance and the slow quasimanifold: some explicit results", *J. Atmos. Sci.* **57**, 1236 (2000).
- Hansen, A.E., Marteau D. and Tabeling, P., "Two-dimensional turbulence and dispersion in a freely decaying system", *Phys. Rev. E* **58**, 7261 (1998).
- Kochin, N.E., Kibel, I.A. and Rose, N.B., *Teoreticheskaya Gidromekhanika*, OGIZ, Leningrad (in Russian) (1948).
- Lovegrove, A.F., Read, P.L. and Richards, C.J., "Generation of inertia-gravity waves in a baroclinically unstable fluid", *Q. J. R. Meteorol. Soc.* **126**, 3233 (2000).
- McIntyre, M.E. and Norton, W.A., "Potential vorticity inversion on a hemisphere", *J. Atmos. Sci.* **57**, 1214 (2000).
- Meleshko, V.V. and van Heijst, G.J.F., "On Chaplygin's investigations of two-dimensional vortex structures in an inviscid fluid", *J. Fluid Mech.* **272**, 157 (1994).
- Pawlak, G. and Armi, L., "Vortex dynamics in a spatially accelerating shear layer", *J. Fluid Mech.* **376** (1998).
- Plougonven, R. and Zeitlin, V., "Internal gravity wave emission from a pancake vortex: an example of wave-vortex interaction in strongly stratified flows", *Phys. Fluids* **14**, 1259 (2002).
- Riley, J.J. and Lelong, M.-P. "Fluid motions in the presence of strong stable stratification", *Annu. Rev. Fluid Mech.* **32**, 613 (2000).
- Saffman, P.G., *Vortex Dynamics*, Cambridge University Press, Cambridge (1992).
- Voropayev, S.I. and Afanasyev, Y.D., "Two-dimensional vortex dipoles interactions in a stratified fluid", *J. Fluid Mech.* **236**, 665 (1992).
- Voropayev, S.I. and Afanasyev, Y.D., *Vortex Structures in a Stratified Fluid*, Chapman and Hall, London (1994).
- Voropayev, S.I., Afanasyev, Y.D. and Filippov, I.A., "Horizontal jets and vortex dipoles in a stratified fluid", *J. Fluid Mech.* **227**, 543 (1991).

